NASA TECHNICAL TRANSLATION

NASA TT F-11,402

NASA TT F-11,402

NUMERICAL CALCULATION OF THE FLOW IN A REGION OF SPHERICAL BLUNTNESS AT SMALL REYNOLDS NUMBERS

V. S. Gorislavskiy and A. I. Tolstykh

Translation of "Chislennyy Raschet Techneniya v Oblasti Sfericheskogo Zatupleniya pri Malykh Chislakh Reynol'dsa." Izvestiya Akademii Nauk SSSR, Mekhanika Zhidkosti i Gaza, No. 5, pp. 93-98, 1967

NATIONAL AERONAUTICS AND SPACE ADMINISTRATION
WASHINGTON, D. C. 20546 MAY 1968

NUMERICAL CALCULATION OF THE FLOW IN A REGION OF SPHERICAL BLUNTNESS AT SMALL REYNOLDS NUMBERS

V. S. Gorislavskiy and A. I. Tolstykh

ABSTRACT: Application of a method used by Tolstykh (1966) and Belotserkovskii (1966) to calculate supersonic flows of a viscous gas past surfaces (circular cylinders) to the calculation of such flows past axisymmetric blunt bodies, at small Reynolds numbers. The aerodynamic characteristics of the flows are obtained under the assumption that the equations of continuum mechanics retain their validity. The results obtained theoretically are compared with those obtained experimentally and with other approximate methods.

References [1, 2] examined the problem concerning the flow around two-dimensional bodies (in particular the circular cylinder) of a hypersonic viscous gas. /93*
Some results for the case of axisymmetric blunt bodies obtained by such methods are cited in this paper. Calculations were carried out to determine the aerodynamic flow characteristics at small Reynolds numbers; it was assumed that the equations of continuum mechanics are applicable. In the case of sufficiently small Reynolds numbers, when the conditions of applicability of the given method may no longer apply, the obtained numerical results are naturally considered as formal. Approximate procedures for the investigation of viscous flow in a region of bluntness [3-5] are available; in these cases, when feasible, a comparison with theoretical results as well as with experimental data is made.

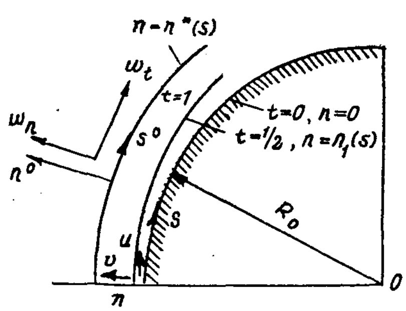

Figure 1.

1. We considered symmetrical hypersonic flow of a viscous, ideal gas around a blunt-body of revolution. As in [1] the initial system of equations is integrated within a region of finite width $0 \leqslant n \leqslant n^*(s)$, where s, n - are the orthogonal coordinates connected with the surface of the body (s is taken from the critical point along the surface; n is taken along the normal to the surface, Fig. 1). This system differs from the Navier-Stokes equations by the absence of some terms of the order O(1/R) and higher and has the form

*Numbers in the margin indicate pagination in the foreign text.

$$
\begin{aligned}
&\frac{\partial}{\partial s}(\rho u)+\frac{\partial}{\partial n}(H\rho v)+j\left(\frac{\rho u}{r}\frac{\partial r}{\partial s}+\frac{H\rho v}{r}\frac{\partial r}{\partial n}\right)=0 \\
&\rho u\frac{\partial u}{\partial s}+H\rho v\frac{\partial u}{\partial n}+k\rho uv=-\frac{\partial p}{\partial s}+\frac{1}{R}\frac{\partial}{\partial n}\left(\mu H\frac{\partial u}{\partial n}\right)- \\
&\quad -\frac{k}{R}\frac{\partial}{\partial n}(\mu u)+\frac{k\mu}{R}\frac{\partial u}{\partial n}+j\frac{\mu H}{Rr}\frac{\partial r}{\partial n}\frac{\partial u}{\partial n} \\
&\rho u\frac{\partial v}{\partial s}+H\rho v\frac{\partial v}{\partial n}-k\rho u^2=-H\frac{\partial p}{\partial n}+\frac{4}{3R}\frac{\partial}{\partial n}\left(\mu H\frac{\partial v}{\partial n}\right)- \\
&\quad -\frac{2}{3R}\frac{\partial}{\partial n}\left(\mu\frac{\partial u}{\partial s}\right)+\frac{1}{R}\frac{\partial}{\partial s}\left(\mu\frac{\partial u}{\partial n}\right)-\frac{7}{3R}\frac{\partial}{\partial s}\left(\mu\frac{ku}{H}\right)+ \\
&\quad +j\left[\frac{\mu}{Rr}\frac{\partial r}{\partial s}\frac{\partial u}{\partial n}-\frac{2}{3R}\frac{\partial}{\partial n}\left(\frac{\mu u}{r}\frac{\partial r}{\partial s}\right)-\frac{\mu k u}{3HRr}\frac{\partial r}{\partial s}-\frac{2\mu u}{Rr^2}\frac{\partial r}{\partial s}\frac{\partial r}{\partial n}\right] \\
&\rho u\frac{\partial}{\partial s}\left(h+\frac{n^2+v^2}{2}\right)+H\rho v\frac{\partial}{\partial n}\left(h+\frac{u^2+v^2}{2}\right)-\frac{1}{\sigma R}\frac{\theta}{\partial n}\left(H\mu\frac{\partial h}{\partial n}\right)+ \\
&\quad +\frac{1}{R}\frac{\partial}{\partial n}\left(\mu H u\frac{\partial u}{\partial n}\right)+\frac{4}{3R}\frac{\partial}{\partial n}\left(\mu H v\frac{\partial v}{\partial n}\right)-\frac{k}{R}\frac{\partial}{\partial n}(\mu u^2)+ \\
&\qquad +j\left(\frac{\mu H}{\sigma H r}\frac{\partial r}{\partial n}\frac{\partial h}{\partial n}+\frac{\mu H u}{Rr}\frac{\partial r}{\partial n}\frac{\partial u}{\partial n}\right) \\
&H=1+kn,\quad p=(\gamma-1)\gamma^{-1}\rho h,\quad R=\rho_\infty w_\infty R_0/\mu_*
\end{aligned}
\tag{1.1}
$$

/94

Here, r(s, n) is the distance between the points (s, n) and the axis of symmetry; μ, ν are the s and n velocity components (Fig. 1), referred to the velocity of the undisturbed flow ω_∞; ρ-is the density, referred to the density of undisturbed flow ρ_∞; ρ-is the pressure, referred to $\rho_\infty \omega_\infty^2$; h-is the enthalpy, referred to ω_∞^2; μ-is the viscosity referred to its value μ_*, when h = 1; the variables s, n, r and curvature k are referred to the radius of curvature at the critical point R_0 and the value $1/R_0$, respectively; R, σ and γ are the Reynolds and Prandtl numbers and the density ratio, respectively; values j = O and j = 1 in the right-hand sides of Eq. (1.1) correspond to the planar and axisymmetrical flows. It is assumed that $M_\infty > 1$, where $M_\infty = \omega_\infty/(\gamma - 1)\ h_\infty$—is the Mach number for the undisturbed flow. The shape of the surface can be sufficiently arbitrary (only the function k, k(s) must be known). However, all concrete calculations were carried out only for the case of spherical bluntness.

Let us dwell on the basis for the selection of an initial system. Equations (1.1) are formally written with an accuracy not lower than 1/R; nevertheless, by means of an a posteriori analysis it is possible to demonstrate that in view of smooth change in functions along the surface of the body, the terms of Navier-Stokes equations not entering into Eqs. (1.1) down to the small values of the Reynolds numbers, play a relatively insignificant role; on the other hand, as indicated below, their absence allows the obtaining of a singular solution of the problem without making use of any information about the subsequent history of the flow. In addition to that, the presence in Eq. (1.1) of all convective terms and terms with higher derivatives with respect to n from the complete system. ensure a sufficiently accurate description of the change in the flow parameters along the normal to the surface. Let us note, that terms with coefficient 7/3, from the right-hand side of the third equation of the system (1.1) are of the order of O (1/R); nevertheless, as calculations have shown, at sufficiently small Reynolds numbers (R < 10), they begin to play a significant role. The "unorthodoxality" of these and several other terms has no particular meaning, since the solution of the system (1.1) is not connected with the construction of any asymptotic expansions in the powers of the Reynolds number.

Let us examine the boundary conditions of the problem. When n = n*, as in the planar case [1], relationships are utilized which were derived from the first approximation equations for the structure of the curvilinear shock-wave (subsequent approximations are of the order of O (1/R) and higher), as well as the relationship determining the line n = n* (s). In the coordinate system (s°, n°), connected with this line (Fig. 1), the boundary conditions have the form

$$\rho w_n = w_{n\infty}, \quad \rho w_n w_t = \frac{\mu}{R}\frac{dw_t}{dn^\circ} + w_{n\infty} w_{t\infty}, \quad \rho w_n^2 + p = \frac{4}{3}\frac{\mu}{R}\frac{dw_n}{dn^\circ} + w_{n\infty}^2 + p_\infty$$
$$\rho w_n\left(h + \frac{w_t^2 + w_n^2}{2}\right) = \frac{\mu}{R\sigma}\frac{dh}{dn^\circ} + \frac{\mu}{R} w_t \frac{dw_t}{dn^\circ} + \frac{4}{3}\frac{\mu}{R} w_n \frac{dw_n}{dn^\circ} + w_{n\infty}\left(h_\infty + \frac{1}{2}\right) \tag{2}$$
$$\frac{dw_n}{dn^\circ} = 0.$$

Here, w_t and w_n are dimensionless s° and n° velocity components; subscript ∞ refers to values of parameters in the undisturbed flow. The last condition determines the position of line n = n* (s) "behind" the shock-wave, which is convenient for the construction of a solution in the region $0 \leqslant n \leqslant n^*$ (s) [the selection of the boundary n* (s) is more practical rather than a matter of principle]. On the surface of the body (n = 0) the usual conditions of adhesion and the temperature conditions are fulfilled /95

$$u = 0, \quad v = 0, \quad \partial n / \partial n = 0.$$

On the axis of symmetry (s = 0) the obvious conditions are fulfilled

$$u = 0, \quad \partial v / \partial s = 0, \quad \partial h / \partial s = 0. \tag{3}$$

In view of the fact that disturbances described by the system (1.1) may be propagated upstream, in order to secure a unique solution of the boundary problem, the conditions for s > 0 are also necessary; these conditions, as in [1], follow from the existence of specific points in the differential equations approximating (1.1)

2. For the numerical integration of Eq. (1.1), scheme 1 of the method of integral relations proposed in [6-7] is utilized; the left-hand sides of Eqs. (1.1) are written down in the divergent form; new functions are introduced:

$$\varphi = \partial u / \partial n, \quad \psi = \partial v / \partial n, \quad \eta = \partial h / \partial n,$$

an equivalent system of first-order equations is integrated termwise from the surface to the limits nj (s) of the region

$$n_0 \leqslant n_{j-1}(s) \leqslant n \leqslant n_j(s) \leqslant n_N, \quad n_0 = 0, \quad n_N = n^*(s), \quad j = 1, \ldots, N$$

into which the total domain $0 \leqslant n \leqslant n^*(s)$ is subdivided. After the substitution of the integrands by interpolation polynomials with interpolation nodes on the boundaries of the regions, the integral expressions are transformed into ordinary differential equations in terms of the desired functions in the nodes. The specific characteristic of the application of scheme 1 remains the same as the planar case. The transformation

$$t(\xi, a) = c\xi + (1-c)\frac{1-\exp(-\xi/a)}{1-\exp(-1/a)} \qquad \left(\xi = \frac{n}{n^*}, \quad c = \text{const}\right) \tag{2.1}$$

causes such an expansion of the region corresponding to the "boundary layer," and such a contraction of the region of "external flow," that the character of change of velocity u and of the expressions related to it become uniform within the entire region $0 \leqslant n \leqslant n^*$. Parameter α, entering into Eq. (1.1) and regulating the degree of expansion of the "boundary layer," depends on the coordinate s and is one of the desired functions. After the transition to the variables s, t, the region $0 \leqslant n \leqslant n^*$ is transformed into a region of constant width $0 \leqslant t \leqslant 1$, while the subdivision of the region of integration into n bands is brought about by lines

$$t_j(\xi_j, a) = j/N \qquad (j = 0, 1, \ldots, N)$$

To the rectilinear calculation network in the fictitious plane (s, t) corresponds a certain nonuniform subdivision in the physical plane (s, n). Moreover, the constant c determines the number of bands in the plane (s, t) corresponding to the boundary layer in the physical plane. The transformation of the type (2.1) permits calculations to be made in a wide range of Reynolds numbers; however, in this paper attention is directed only to regions of small Reynolds numbers, consequently, c is assumed to be equal to zero.

In constructing the interpolation polynomials in t for the functions $u, v, p, h, \varphi, \psi, \eta, \mu$ and groups ρu^2, ρuv, $\rho u(h + {}^1\!/_2 u^2 + {}^1\!/_2 v^2)$, the character of their behavior near the surface is taken into account. The sum of the highest powers of all polynomials is taken to be one less than the corresponding sum of the usual approximation in the physical plane. This is related to the introduction of the parameter a as an unknown function.

For the purpose of closing the system of integral equations, boundary conditions (1.2) are used; these conditions are written in the system of coordinates (s, n) and are represented in the form of equations with the independent variable s. Noting that

$$d\varepsilon/ds = (1 + k\varepsilon)\,\mathrm{tg}\,\tau$$

(where $\epsilon = n^*$, τ is the slope of the line $n = n^*$ in the direction of the undisturbed flow), the approximating system is finally recorded in the form

$$S(z, s)\,dz/ds = b(z, s) \tag{2.2}$$

where S is the matrix, b is the vector of the right-hand side whose components are the unknown functions $u_i, v_i, p_i, h_0, h_i, a, \varepsilon, \tau$ $(i = 1, \ldots, N)$; the subscript refers to the number of bands taken from the body $(u_0 = v_0 = 0)$. Pressure on the surface of the body does not enter into Eq. (2.2), and is determined from

$$p_0 - \frac{\gamma - 1}{\gamma} h_0 \frac{(\rho u)^2_{t=0}}{(\rho u^2)_{t=0}}$$

The system (2.2) is analogous to the corresponding system for the planar case and is distinguished from it only by the presence of additional terms, mainly in the components of vector B; the fairly complex expressions for matrix S and vector components are not cited here. /96

The boundary conditions for Eq. (2.2) when S = 0, follow from the conditions of symmetry (1.3). After the presentation of components of vector Z in the form of a series of even and odd powers of s of Eq. (2.2); these are converted into systems of algebraic equations with respect to the coefficient of expansion. These systems are shown to be unclosed; in the N-th approximation N parameters remain indeterminate. Unknown parameters are found from conditions of regularity in N specific points - as in the planar case [1]. In this manner we obtain the boundary problem for the system (2.2); its solution involved multiple integration of equations from the axis of symmetry with checking whether the conditions for the specific points have been fulfilled. Departure from the axis of symmetry was accomplished by using the first terms of the expansion in the neighborhood s = 0, with known parameters $\alpha(0)_3$ $\epsilon(0)$ for N = 2 and $\alpha(0)$, $\epsilon(0)$, $\nu j(0)$ (j = 2..., N-1) for n > 2.

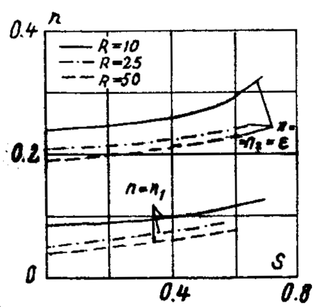

Figure 2.

3. The calculations were carried out on a digital computer, using a program for an arbitrary number of approximations ($N \geq 2$); the convergence of methods was not investigated and all data were obtained for N = 2. It was assumed that viscosity changes according to the law μ M h 1/2.

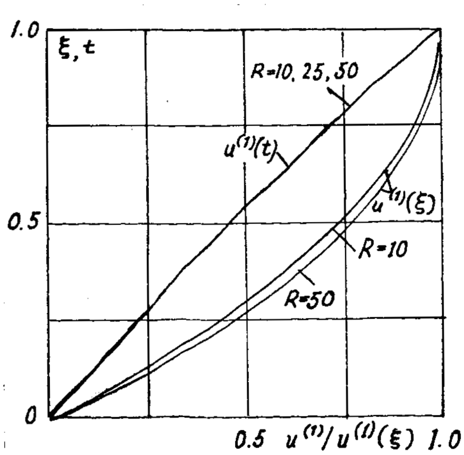

Figure 3.

The following parameters of undisturbed flow were assumed $M_\infty = 10$, $\sigma = 0.72$; $\gamma = 7/5$, in addition, for the purpose of comparison with the results of [4] the value $\nu = 5/3$ was employed in one case. Correspondence between the physical plane and plane (s, t) is evident from Fig. 2, where for different values of the numbers R, the boundaries of bands nj(s) are determined by lines tj = j/N(j = 1, 2).

For the comparison of longitudinal velocity profiles in the fictitious and physical planes, functions $u^{(1)}(t)$ and $a^{(1)}(\xi)$ $(u^{(1)})$ are plotted in Fig. 3 (the coefficient in the expansion $u = u^{(1)}s + O(s^3)$, determines the character of velocity change in the greater part of the region of integration). In accordance with the purpose of transformation (2.1), function u(t) is almost linear, and within the range of Reynolds numbers under discussion, it has a universal character.

Typical distribution of flow parameters along the axis of symmetry is shown in Fig. 4 ($\gamma = 5/3$, $R = 20$); dotted lines represent data of approximate theory [4] for the case of the heat-insulated surface, obtained for approximately the same values of numbers R and σ ($M_\infty = 10$, $\nu = 1/3$, $\mu = h^{1/2}$).

In view of the difference in the width of the shock-layer (in the given work $\epsilon \approx 0.3$, in [4] $\epsilon \approx 0.2$, if under ϵ in the second case, we understand the distance on which the velocity ν coincides with magnitude $\nu(\epsilon)$ in the first case), instead of coordinate n, $\epsilon = n/\epsilon$ was used.

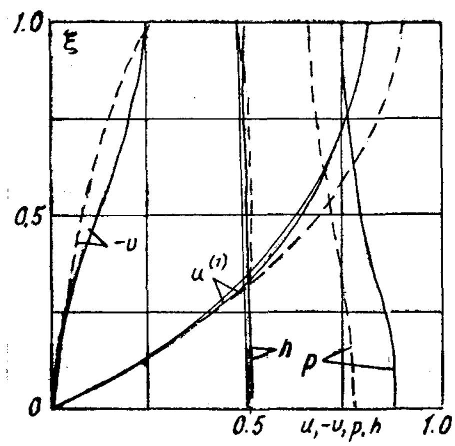

Figure 4.

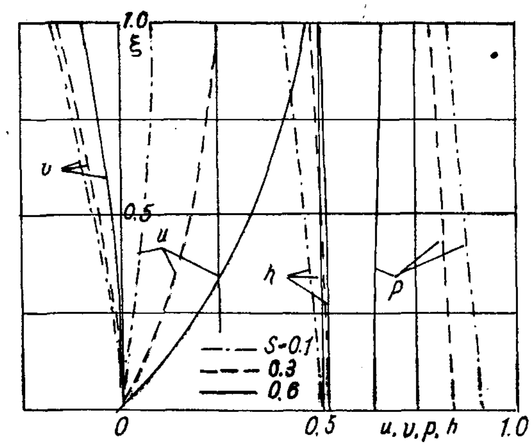

Figure 5.

Typical variation of flow parameters along the normal to the surface at different values s is illustrated in Fig. 5 ($R = 10$); all distributions along n as well as when s = 0 were obtained by means of interpolation polynomials.

Calculations have shown, that with a decrease in the Reynolds number, velocity, pressure and enthalpy profiles undergo an insignificant change: the basic effect of the rarefaction within the medium is manifested by a considerable increase in the width of the shock-layer. In Fig. 6 the change in pressure, enthalpy and friction on the surface of the sphere is represented in the form of functions $p_0(s)/p_0(0)$, $H_0(s)$ and $c_j(s)$ [$c_j = 1/R\,(\mu \partial u/\partial n)_{n=0} = \mu_0 \varphi_0/R$. Dotted lines traced in the same figure represent curves, corresponding to the limiting cases $R = \infty$ pressure on the sphere in the flow of an ideal gas $M_\infty = 10$, $\gamma = 1.4$ [8] and $R = 0$ coefficient of friction drag in free molecular flow $c_j°$, diffusion reflection, coefficient of accomodation is equal to unity.

Let us examine the function $p_0(s)$; as is evident from Fig. 6, the ratio /97
$p_0(s)$ $p_0(0)$ depends little on the Reynolds number and does not differ greatly from its value in the flow of an ideal gas. However, the value $p_0(0)$ at small values of R begins to increase appreciably with an increase in the rarefaction of the medium. In the Fig. 7 we find the function $p_0(0)/p_{0i} = P(R)$

along with the experimental data [9, 10] (cross-hatched areas); here p_{0i} is the value of $p_0(0)$ for an ideal gas. Dotted lines represent the results obtained in [4], for $\gamma = 5/3$.

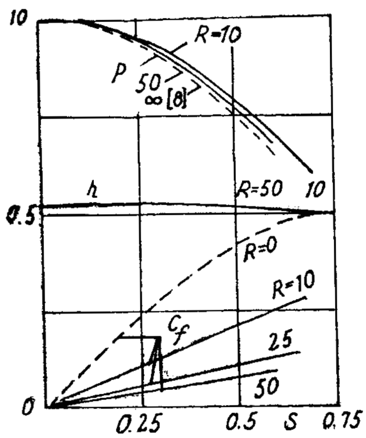

Figure 6.

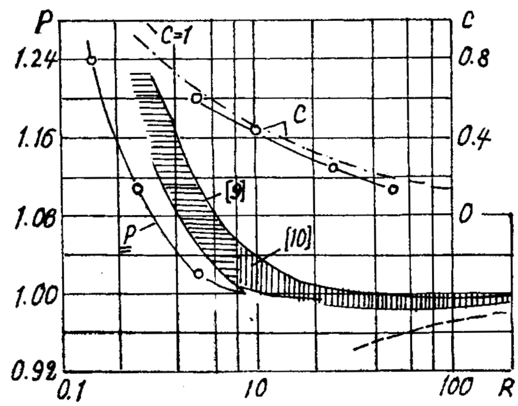

Figure 7.

Estimated values of P, for $10 \leqslant R \leqslant 50$ are proven to be somewhat smaller than 1, which corresponds to the experimentally established value [10]; when $R < 10$ the theoretical curve is of the same shape as the experimental curve function; however, it passes slightly to the left of the experimental curve (it is possible that the Reynolds numbers in the given work and the measured Reynolds numbers were not equivalent). In converting the Reynolds numbers from [10] we used $\mu \sim h^{\omega}$, $\omega = 1/2$; in case of $\omega > 1/2$ the experimental points of Fig. 7 shift to the left, and agreement between the theoretical and experimental data appears to improve. Let us note that the calculated data well approximate the single-parameter curve passing through P when R=O in free molecular flow (p/o) = 1.64, when $\gamma = 7/5$:

$$P \approx 0.99 \times (P(0) - 0.99 \exp(-0.65R)$$

Dependence of the coefficient of friction drag on the Reynolds numbers may be characterized by $C = (c_f / c_f^0)_{s=0}$; function C/R is illustrated in Fig. 7 by the curve c = 1.47R1/2 is also shown by dash-dotted line on the same figure, this curve was obtained for the boundary layer on blunt body for $\gamma = 7/5$ from formulas used in [3]. Let us note, that if we take an interest in values of $p_0(0)$, it is sufficient to select only rough values of initial parameters. For example, as /98
was shown through numerical experiments, $\partial p_0(0) / \partial t(0) \approx 0.1$ and $\partial p_0(0) / \partial \alpha(0) \approx 0.001$ $(1 \leqslant R \leqslant 50)$. This fact was utilized in constructing the theoretical curve P/(R) in Fig. 7 for R < 5.

REFERENCES

1. Tolstykh, A.I. Numerical Calculation of the Hypersonic Flow-Around Blunt-Bodies by a Biscous Gas. Jl. of Comp. Math. and Math. Phys. 1966, Vol. 6, No. 1, pp. 113-120.

2. Belotserkovskii, O.M. Flow-Around Blunt-Bodies by Hypersonic Flow of a Viscous Gas. Ed. "World", 1964, p. 58.

3. Ho, H. T., Probstein, R. F. The Compressible Viscous Layer in Rarefied Hypersonic Flow. Rarefied Gas Dynamics, Academic Press, 1961, pp. 525-552.
4. Yosikhim, H., Levinski, E. Flow-Around a Sphere by a Hpersonic Flow of a Rarefied Gas. Ed. "World", 1964, pp. 58.
5. Cheng, H. K. The Blunt-Body Problem in Hypersonic Flow at Low Reynolds Number. JAS Paper, 1963, pp. 63-92.
6. Dorodnitsyn, A. A. Method of Numerical Solution of Some Nonlinear Problems, of Aerodynamics. Transactions III, All-Union Math. Conf., 1956, Vol. 3, AN SSSR, 1958.
7. Belotserkovskii, O. M. The Symmetrical Flow-Around Blunt-Bodies by Hypersonic Flow of an Ideal and Real Gas. J. of Comp. Math and Math. Phys. 1962, Vol. 2, No. 6, pp. 1062-1085.
8. Belotserkovskii, O. M. Calculation of the Flow-Around Axisymmetric Bodies of a Receding Shock-Wave. Vts. AN SSSR, 1961.
9. Sukhnev, V. A. On the Determination of Corrections for the Reading of Settings Under Full Pressure in Hypersonic Flow of a Rarefied Gas. Izvestiya AN SSSR, Mekhanika i Mash., No. 5, 1964.
10. Potter, J. L. The Transitional Rarefied Flow Regime. Paper Presented at the Fifth International Symposium on Rarefied Gas Dynamics, Oxford, England, 1966, July.

Translated for the National Aeronautics and Space Administration by Scripta Technica, Inc., NASw-1694.